Formation of inner-shell autoionizing CO^+ states below the CO^{++} threshold

T. Osipov,[1] Th. Weber,[1] T. N. Rescigno,[1] S. Y. Lee,[1] A. E. Orel,[2] M. Schöffler,[1] F. P. Sturm,[1,3] S. Schössler,[3] U. Lenz,[3] T. Havermeier,[3] M. Kühnel,[3] T. Jahnke,[3] J. B. Williams,[4] D. Ray,[5] A. Landers,[4] R. Dörner,[3] and A. Belkacem[1]

[1]*Lawrence Berkeley National Laboratory, Chemical Sciences, Berkeley, CA 94720, USA*
[2]*Department of Applied Science, University of California, Davis, CA 95616, USA*
[3]*Institut fur Kernphysik, Universitat Frankfurt, D-60438 Frankfurt, Germany*
[4]*Department of physics, Auburn University, Auburn, AL 36849, USA*
[5]*J. R. Macdonald Laboratory, Kansas State University, Manhattan, KS 66506, USA*

We report a kinematically complete experiment on the production of CO^+ autoionizing states following photoionization of carbon monoxide below its vertical double ionization threshold. Momentum imaging spectroscopy is used to measure the energies and body-frame angular distributions of both photo- and autoionization electrons, as well as the kinetic energy release (KER) of the atomic ions. This data, in combination with *ab initio* theoretical calculations, provides insight into the nature of the cation states produced and their subsequent dissociation into autoionizing atomic (O^*) fragments.

PACS numbers: 33.80.Eh

Because of the long-range repulsive Coulomb interaction between singly charged ions, the vertical double ionization thresholds of small molecules generally lie above the dissociation limits corresponding to formation of singly charged fragments. This leads to the possibility of forming singly charged molecular ions by photoabsorption in the Franck-Condon region at energies below the lowest dication state, but above the dissociation limit into two singly charged fragment ions. These singly charged molecular ions can emit a second electron by autoionization, but only at larger internuclear separations where the ionic state crosses into the electron+dication continuum. This process has been termed indirect double photoionization and was observed some time ago in H_2O by Winkoun *et al.* [1] and in CO by Lablanquie *et al.* [2] and has continued to attract the attention of theorists and experimentalists alike. Much of this work has focused on identification of the atomic (generally oxygen) autoionizing states which are populated in the indirect double photoionization process [3, 4], but comparatively less is known about the character of the singly ionized states initially produced [5]. This is hardly surprising since the independent-particle (Koopmans') description generally breaks down for inner-valence singly charged ions. Since these states are characterized by strong configuration mixing and numerous curve crossings [6], the inner valence regions of molecular ions continue to be a challenging subject both experimentally and theoretically.

In this work, single CO molecules were irradiated with a 43 ±.010 eV beam of soft x-rays from the Advanced Light Source. A COLTRIMS (COLd Target Recoil Ion Momentum Spectroscopy) [7] setup was used to perform a kinematically complete experiment by measuring the 3D momenta of all fragments - photo- and autoionization electrons as well as the C^+ and O^+ ions - in coincidence. The setup is similar to the one described in ref. [8]. In brief, the focused linearly polarized photon beam is crossed with a supersonic beam of CO molecules. Electrons and ions created in the interaction volume are guided by an electrostatic field of 4 V/cm and a parallel homogeneous magnetic field of 4.5 Gauss towards two 80 mm diameter large active area sensitive channel plate detectors equipped with delay-line position readout [9]. Additionally, McLaren-type time focussing was employed on the electron and the ion arm of the spectrometer. The length of the drift regions on both sides of the interaction volume are designed to yield 4π solid angle collection for electrons up to 6 eV and ion KER up to 6 eV.

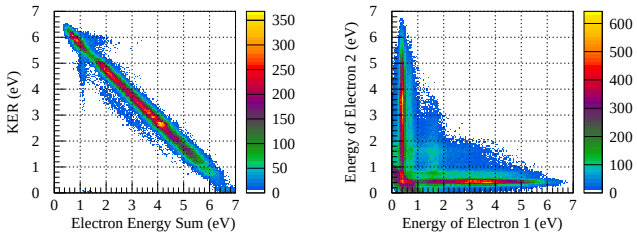

FIG. 1: (Color online) Left: 2D plot of the sum energy of the two electrons versus the translation energy of the ion fragments. Photon energy is 43 eV. Right: two dimensional plot of the energy of one electron versus the second electron. The figure is symmetric, but not mirrored, with respect to a 45 degree line passing through the origin. The intense vertical and horizontal lines correspond to monoenergetic autoionization electrons.

The total energy of the photon will be divided among the two electrons, the ion translational energy and the final asymptotic energy of the dissociated fragments. In Fig. 1 we show the sum energy of the electrons (horizontal axis) versus the kinetic energy release (KER) of the fragment ions (vertical axis). The intense 45° line has a KER asymptote of ≈7 eV corresponding to an asymp-

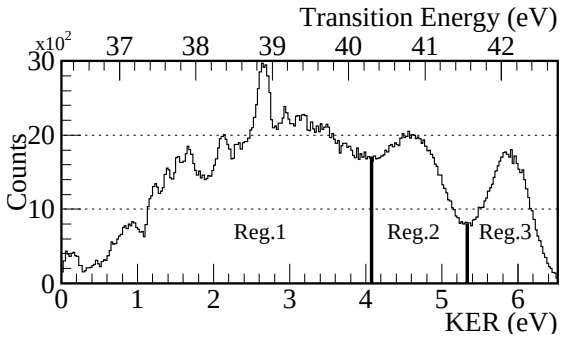

FIG. 2: KER spectrum of the ion fragments. There is a one-to-one correspondence between the kinetic energy release and the transition energy to the excited CO^{*+} in the Franck-Condon region.

totic fragment energy of 36 eV (43 eV photon energy -7 eV) for the dissociated molecular dication $C^+ + O^+$. This asymptotic energy corresponds to having both ions in their ground states. We observe that there is marked structure along the intense line in the 2D plot. With the exception of the little island at the top left corner in the plot, which corresponds to direct double ionization through low-lying states of CO^{++}, all the states that are populated vertically in the Franck-Condon region are highly excited cationic states that lie below the lowest state of the dication but above the asymptotic limit of $C^+ + O^+$ in their ground states. In other words, the majority of the dissociation to the asymptotic dication $C^+ + O^+$ starts in the Franck-Condon region as a highly excited cation CO^{*+}. Indirect double ionization proceeds through an autoionization process. This is clearly seen in the right panel of Fig. 1 where we plot the energy of one electron versus the energy of the other. One observes predominant vertical (or horizontal) lines that correspond to monoenergetic autoionization electrons; we have confirmed their energy to be independent of photon energy. This observation is in good agreement with the observations reported in ref. [4]. Note that the electron resolution in the present experiment is about 100 meV, thus easily separating the lines at 0.5 eV, 0.8eV and 1.7 eV, but is insufficient to resolve the substructure in the lines themselves, as done in ref. [4].

Figure 1 shows a linear dependence between the sum energy of the two electrons (photoelectron + autoionization electron) and KER. In this experiment we measure the kinetic energy release with better resolution than the electron energy. Making use of this better resolution, we show in Fig. 2 the kinetic energy release spectrum obtained by projecting the data in Fig. 1 (left panel) onto the KER axis. There is also a linear dependence between KER and the vertical transition energy to excited CO^{*+} in the Franck-Condon region, which is shown at the top horizontal axis. The KER spectrum exhibits three broad regions. Region 1, with KER less than 4 eV (or below 40 eV for the transition energy) exhibits marked structure with discrete peaks. Region 2, with KER between 4 and

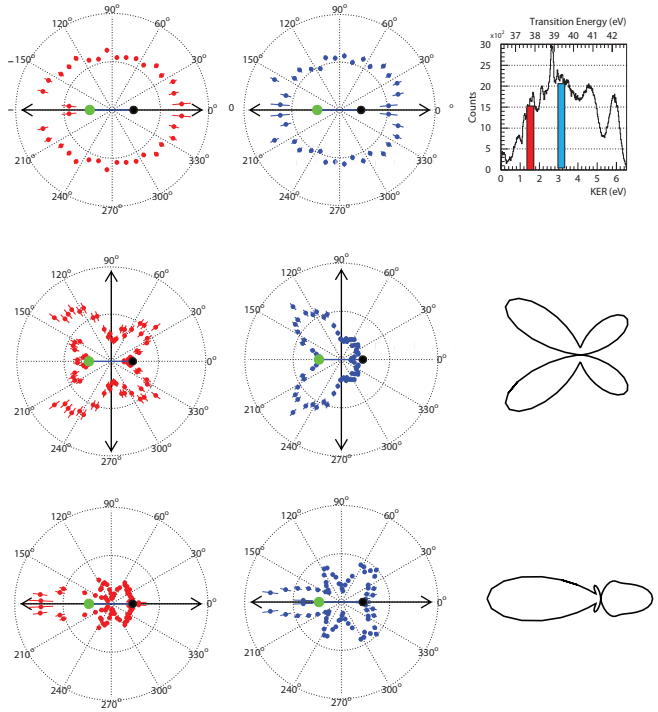

FIG. 3: (Color online) Molecular-frame photo- and autoionization electron angular distributions for indirect double ionization of CO in region 1. The molecule is oriented horizontally with the oxygen located on the left. The energy bands selected are shown in the KER spectrum in the top right panel. Left column: 37.5 eV band; middle column: 39.3 eV band. Autoionization distributions are shown in the two top panels. Middle row : measured and calculated MFPADs for perpendicular photon polarization. Bottom row: measured and calculated MFPADs for parallel polarization.

5 eV, is characterized by a broad smooth peak. Region 3, with KER greater than 5 eV and transition energies above 41.5 eV, corresponds to the direct double ionization region. We find the distributions of photoelectrons produced in regions 1 and 2 to be markedly different. In order to gain insight into the electronic states that are involved in these two regions we will present below the molecular-frame photoelectron angular distribution measured in regions 1 and 2 for photon polarization both parallel and perpendicular to the molecular axis.

Figure 3 shows measured photo- and autoionization electron angular distributions in region 1 taken with 43 eV photon energy. The measured values displayed include distributions from electrons in ≈0.5 eV bands centered near transition energies 37.5 eV and 39.3 eV, corresponding to photoelectron energies of 5.5 eV and 3.7 eV, respectively. We believe that the region 1 data supports the assumption that among the initially produced CO^+ ions are two inner-valence states created by removal of a 3σ (O 2s) electron. This interpretation is at odds

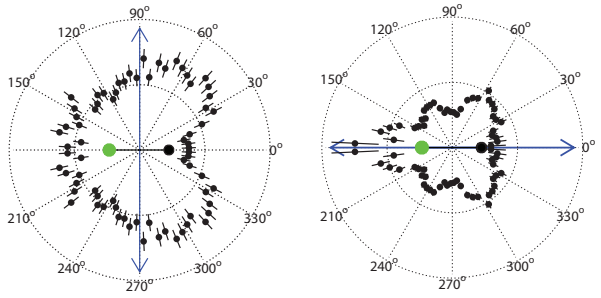

FIG. 4: (Color online) Measured MFPADs for indirect double ionization of CO in region 2. Data plotted is for an ≈.5 eV band at 40.8 eV. Left: perpendicular photon polarization; right: parallel polarization. The molecule is shown horizontal with the oxygen located on the left.

with that reached by Hikosaka *et al.* [3], who concluded that the CO^+ states in the 38 eV region must be Rydberg states associated with the low-lying CO^{++} dication states, since they support discrete vibrational levels, in contrast to the inner-valence ion states which were assumed to be purely dissociative. The latter assumption was based on earlier theoretical calculations by Baltzer *et al.* [10] who found all valence excited CO^+ states above 30 eV to be dissociative.

The first piece of theoretical evidence that supports an inner-valence CO^+ state mechanism comes from calculations of the molecular-frame photoelectron angular distribution (MFPAD) for 3σ ejection. We obtain photoionization amplitudes from *ab initio* calculations using a single configuration Hartree-Fock wave function for the neutral CO target and a final continuum state computed at the single-channel static-exchange level by using neutral orbitals to describe a CO^+ ion with a 3σ vacancy. We used the complex Kohn variational method to generate the molecular continuum wave functions [11, 12]. The basis sets employed here are the same as those used in our earlier calculations on valence photoionization of CO [11]. The calculations were performed at the equilibrium internuclear separation of neutral CO (1.13Å).

Figure 3 shows our calculated MFPADs, which were carried out at 4.0 eV photoelectron energy. Results are shown for linear photon polarization both parallel and perpendicular to the molecular axis. The photoelectron angular distributions shown in the two lower rows of Fig. 3 exhibit very characteristic lobes that can be directly compared to the theoretical calculations. Evidently, the calculated photoelectron distributions are in reasonably good agreement with the measured values. For parallel polarization, theory and experiment both show a propensity for photoejection along the molecular axis directed toward the oxygen side of the molecule, as well as minor lobes near ±60° from the CO axis. For perpendicular polarization, theory and experiment both show a four-lobed photoelectron angular distribution, with a propensity for ejection again on the oxygen side.

The angular distributions of the autoionization electrons, shown at the top of Fig. 3 for horizontal polarization, are featureless. This is very different from the situation reported [13] for dissociation of O_2 into O+O* by 22.36 eV photons, which produces asymmetric autoionization electron distributions, and it implies that in the present case the atomic autoionization is taking place at large internuclear separation, in line with the results of our calculations discussed below.

Figure 4 shows measured parallel and perpendicular angular distributions in region 2 for photoelectrons correlated with the C^+ + O^+ channels, again with 43 eV photon energy but for photoelectrons associated with the band near 40.8 eV transition energy. These distributions are strikingly different from the region 1 data shown in Fig. 3, suggesting that this band does not arise from an inner-valence CO^+ excited state, since the changes occur over a very narrow range of energy (less than 0.5 eV wide) at the border of the two regions (40.2 eV). The difference is particularly visible in the perpendicular polarization. In region 2 the two prominent lobes point to the carbon side (right), while over a broad range spanning all of region 1, the two lobes point to the oxygen side . Photoionization in region 2 most likely involves excitation of a number of closely spaced Rydberg CO^+ states just below the threshold for direct double ionization. This will be further discussed in a separate publication.

Attempts to theoretically characterize inner-valence CO^+ states are complicated by the fact that the states above 30 eV show strong mixing between $3\sigma^{-1}$, doubly-excited valence and Rydberg configurations. The potential energy curves resulting from a "brute-force" approach to the problem show numerous crossings and, in the absence of detailed non-adiabatic couplings, it is difficult to determine which crossings are avoided. We therefore opted for a more intuitive approach to the problem, with a set of restricted configuration-interaction (CI) calculations designed to highlight the essential inner-valence/Rydberg mixings. A molecular orbital basis for the calculations was constructed from a triple-zeta set of contracted Gaussian functions for both C and O [14], augmented with additional s- and p-type functions (orbital exponent=0.03) on the oxygen. First we perform a complete-active-space multi-configuration self-consistent field (MCSCF) calculation on the $^3\Pi$ state of CO^{++}, which generates ten reference orbitals. To this set we added oxygen atomic-like 3s and 3p orbitals by orthogonalizing the diffuse oxygen-centered Gaussians to the other reference orbitals. The virtual orbital space includes a complementary set of functions constructed from the original set of contracted Gaussian functions. For the CI calculations on CO^+, a set of reference configurations associated with the inner-valence states is generated by singly-occupying the 3σ orbital and distributing the other 12 electrons over the remaining 9 MCSCF orbitals. A corresponding set of Rydberg configurations is chosen by singly-occupying a diffuse oxygen orbital and distributing the remaining electrons among the MCSCF orbitals,

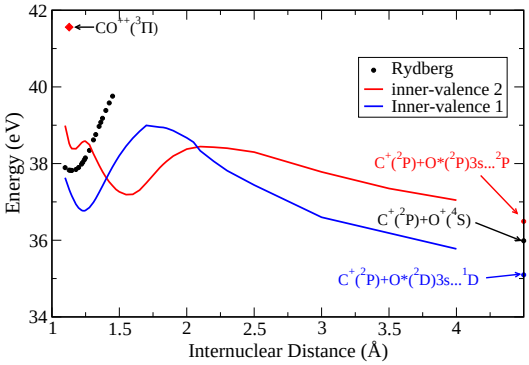

FIG. 5: (Color online) Calculated CO^+ potential energy curves.

keeping the 3σ orbital doubly occupied. We then include single excitations from the reference configurations into the virtual orbital space, with the restriction that there never be more than one electron in a diffuse orbital. In all configurations, the core O and C 1s orbitals were kept doubly-occupied. With this prescription, the CI calculations, which were performed in C_{2v} symmetry, included ∼21,000 configurations in overall $^2A_1$ symmetry. A similar prescription for calculations on the $^3\Pi$ ground-state of CO^{++} gives ∼12,500 configurations.

The calculated CO^+ potential curves relevant to this discussion are plotted in Fig. 5. The point at R=1.13Å near the top is our calculated value for the $^3\Pi$ ground-state of CO^{++}, which we place at 41.56 eV, relative to the equilibrium value of neutral CO, based on the accurate calculations of Eland *et al.* [15]. There are numerous crossings among the calculated CO^+ states. To arrive at the plotted curves, we examined the dominant CI coefficients as a function of R, allowing states to cross if there was little interaction, but following the adiabatic curve otherwise [6]. We do find two $^2\Sigma^+$ CO^+ states with predominantly $3\sigma^{-1}$ character in the Franck-Condon region, shown as solid curves in Fig. 5. At R=1.13Å, their transition energies are 37.3 and 38.5 eV, respectively, which places them both within region 1. The $3\sigma^{-1}$ character of both states decreases with increasing R as they take on more O 3s Rydberg character. The upper inner-valence state correlates directly with C^+,^2P + autoionizing $O^*(2p^3(^2P)3s)$,^3P. Its double-well structure and the deep well centered near 1.5 Å suggest that its parent dication state is the excited $d^1\Sigma^+$ state of CO^{++} [15]. The lower inner-valence state correlates to C^+ + $O^*(2p^3(^2D)3s)$,^1D, which is below the dication asymptote. However, the two states cross near 1.4Å and 2.1Å, so both states could feed the O^* autoionizing state. Finally, the calculations also show a Rydberg CO^+ state of $^2\Sigma^+$ symmetry, whose parent dication is the lowest $^3\Sigma^+$ state of CO^{++}, that lies between the two inner-valence states. Photoionization which populates the lower vibrational levels of this state could explain the sharp features that overlay the region 1 background.

In summary, we believe that the broad indirect double ionization band in CO centered about 39 eV is initiated by creation of inner-valence $3\sigma^{-1}$ CO^+ states that dissociate to C^+ + O^* fragments. The most compelling evidence for this assignment comes from a comparison of our measured and theoretically calculated molecular-frame photo-electron angular distributions. Further evidence is provided by multi-reference configuration-interaction calculations which show two $^2\Sigma^+$ CO^{+*} states with oxygen 2s-hole character in the Franck-Condon region. These states take on predominantly Rydberg character at larger internuclear distances. The calculations also suggest that population of vibrational levels of an electronically excited Rydberg CO^+ state may well explain the discrete bands seen in the experimental data. Finally, an elementary calculation based on the ≈0.5 eV energy difference between autoionizing O^* and ground-state O^+ and the asymptotic shapes of the CO^{+*} (flat) and CO^{++} (1/R) potential curves suggests that CO^{+*} can only autoionize at internuclear distances larger than 25 Å, making it an ideal candidate for two-color pump-probe experiments with ultrashort-pulse, soft x-ray lasers. The results presented here will aid in the interpretation of current and planned pump-probe experiments aimed at further characterizing the time-dependence of indirect double ionization.

This work as performed under the auspices of the US DOE under contract DE-AC02-05CH11231 and supported by the US DOE Office of Basic Energy Sciences, Division of Chemical Sciences. Support by DAAD and DFG are gratefully acknowledged. Author M.S. thanks the Humboldt-foundation for financial support.

[1] D. Winkoun, G. Dujardin, L. Hellner, and M. Bernard, J.Phys. B **21**, 1385 (1988).
[2] P. Lablanquie, *et al.*, Phys. Rev. A **40**, 5673 (1989).
[3] Y. Hikosaka, *et al.*, J. Electron Spectrosc. Rel. Phen. **125**, 99 (2002).
[4] Y. Hikosaka and J. H. D. Eland, Chem. Phys. **299**, 147 (2004).
[5] A. S. Sandhu, *et al.*, Science **322**, 1081 (2008).
[6] M. A. Hayes and C. J. Noble, J. Phys. B **31**, 3609 (1998).
[7] J. Ullrich et al, Rep. Prog. Phys. **66**, 1463 (2003).
[8] T. Jahnke, *et al.*, Phys. Rev. Lett. **93**, 083002 (2004).
[9] O. Jagutzki, *et al.*, Nuc. Instr. Meth. **A477**, 244 (2002).
[10] P. Baltzer, *et al.*, J. Phys. B **27**, 4915 (1994).
[11] T. N. Rescigno, B. H. Lengsfield III, and A. E. Orel, J. Chem. Phys. **99**, 5097 (1993).
[12] S. Miyabe, C. W. McCurdy, A. E. Orel, and T. N. Rescigno, Phys. Rev. A **79**, 053401 (2009).
[13] A. V. Golovin, *et al.*, Phys. Rev. Lett. **79**, 4554 (1997).
[14] T. Dunning, J. Chem. Phys. **53**, 2823 (1970).
[15] J. H. D. Eland, *et al.*, J. Phys. B **37**, 3197 (2004).